Smart Agricultural Technology 3 (2023) 100067

Contents lists available at ScienceDirect

Smart Agricultural Technology

journal homepage: www.elsevier.com/locate/atech

Evaluating biostimulants via high-throughput field phenotyping: Biophysical traits retrieval through PROSAIL inversion

Giulia Antonucci[a,1,*], Giorgio Impollonia[a,b,1], Michele Croci[a,b], Eleonora Potenza[a], Andrea Marcone[a,b], Stefano Amaducci[a,b]

[a] Department of Sustainable Crop Production, Università Cattolica del Sacro Cuore (UCSC), Piacenza, 29122, Italy
[b] Remote Sensing and Spatial Analysis Research Center (CRAST), Università Cattolica del Sacro Cuore, Piacenza, 29122, Italy

ARTICLE INFO

Keywords:
Water stress
Biostimulant
PROSAIL
GAM
UAV
Tomato
LCC

ABSTRACT

Drought management largely depends on the availability of timely, accurate and integrated information about its characteristics. Concurrently, biostimulants could represent a sustainable measure to foster the resilience of cropping systems under water-limited conditions. Nevertheless, scientific recognition of the potential of biostimulants has not grown as fast as the interest from industry: therefore, there is an urgent need to investigate biostimulant action. In recent decades, remote sensing has been successfully applied to crop growth and stress monitoring. The use of radiative transfer models, often rooted in artificial intelligence, to estimate plant traits from remotely sensed data can be considered the link between the generalisation and the spatialisation of data, bringing field phenotyping and remote sensing closer together. In this framework, the present study was designed as a factorial combination of irrigation treatment (3 levels) and biostimulant treatment (3 levels) and conducted on processing tomato in open field during the summer of 2020. PROSAIL inversion was carried out to retrieve three major biophysical traits (LAI, LCC, CCC). The parameters dynamics during the season were investigated through GAM modelling. The validation of the model was carried out with a positive outcome in terms of accuracy. The PROSAIL inversion enabled the efficient retrieval of LAI and LCC at rates comparable to those in literature, while performing worse than literature findings only for CCC, probably due to the characteristics of tomato canopy. At the same time, the effect of irrigation was detected both for yield and quality data and detected through the GAM modelisation of the parameters. However, no biostimulant effect could be detected. The internal variability per plot of the retrieved biophysical traits was high. This, jointly with the uncertainty surrounding biostimulant testing and the magnitude of biostimulant effects, corroborated by the absence of results regarding biostimulant effect on yield and DM, lead to hypothesise that the bottleneck was linked to the biostimulant effect itself.

1. Introduction

Drought is recognised as one of the major negative factors affecting agricultural production. In this context, drought management represents a key strategic tool to achieve sustainable agriculture while minimising drought-related losses of crop plant productivity. Its management largely depends on the availability of timely, accurate and integrated information about its characteristics [1].

Biostimulants, as pointed out by Del Buono [2], could represent a sustainable measure to foster the resilience of cropping systems under water-limited conditions. Plants' first response to drought is represented by stomatal closure, which then results in the inhibition of photosynthesis [3] and therefore leads to CO2 uptake and concentration reduction [4], leading to a lower accumulation of biomass. Among biostimulant constituents, osmolytes targeting water stress resistance in plants, such as glycinebetaine (GB), are rising in application. GB acts in multiple ways in order to contrast water stress: as an osmoregulator; by stabilising structures and activities of enzymes and protein complexes via detoxification of reactive oxygen species [5,6]; by maintaining the integrity of membranes against the damaging effects of excessive salt [7–10], cold [11], heat [12,13] and freezing [14,15], as well as drought [16]. The role of GB in plant resistance to abiotic stressed has been widely investigated and documented [17–21]. Nevertheless, scientific recognition of the potential of biostimulants has not grown as fast as the interest from industry [22]: this has been caused by limited fundamental research of their modes of action and the high speed at which new multi-compound products have entered the market. Therefore, there is an urgent need to investigate biostimulant action. In this context, the

* Corresponding author
E-mail address: giulia.antonucci@unicatt.it (G. Antonucci).
[1] These authors contributed equally to this work.

https://doi.org/10.1016/j.atech.2022.100067
Received 8 March 2022; Received in revised form 10 May 2022; Accepted 10 May 2022

necessity of accurate assessment of phenotypic variables is emerging as a critical issue [23]. In this context, emerging digital technologies such as sensors, automatic image acquisition and the connected algorithms and models have seen an increasing adoption.

In recent decades, remote sensing has been successfully applied to crop growth and stress monitoring [24–26]. The use of unmanned aerial vehicles (UAVs) in particular has been on the rise: representing an economical and efficient method to meet the increasing requirements of spatial, temporal, and spectral resolutions [27–30], they are able to provide flexible high information resolution.

As of today, thermal UAV is mainly employed in detecting drought stress: the most common drought stress signals in plants (i.e. temperature) are susceptible to detection by thermal camera technology, namely by exploiting the inverse linear relation between transpiration and surface temperature of leaves [31,32].

Remote sensing represents a highly flexible and widely used instrument to assess various plant traits. Nevertheless, the assessment of complex traits such as the identification and quantification of abiotic and biotic stress is still regarded as challenging: there is a rising necessity to establish reliable retrieval techniques enabling the spatiotemporally explicit quantification of biophysical traits. Among others, precision agriculture [33,34], crop phenotyping [35], monitoring of crop traits [36,37] and the improvement of yield prediction [38,39] all rely on the possibility to quantitatively estimate bio-physical/-chemical crop parameters accurately [40]. Remote sensing in particular, and spectroscopy data at large, are suited for the cost-effective estimation of biophysical plant traits through the dense information content contained in few spectral bands, either narrow or broad (Verrelst et al., 2019).

While remote sensing approaches in the past have mainly involved hyperspectral cameras [34,40–45], crucial biophysical traits such as leaf area index (LAI) have also successfully been retrieved through the use of multispectral cameras. Among multiple parameters that can be retrieved, leaf area index (LAI) is of particular interest: a key canopy structural variable, it is used in order to model crop growth [46,47], yield variability [48], monitor crop growth [49], predict the crop yield [50], estimate the amount of aboveground biomass [27], and evaluate the effects of field management [51]. At the same time, chlorophyll content, defined either at the leaf level (leaf chlorophyll content, LCC) or at the canopy level (canopy chlorophyll content, CCC) is used as a bioindicator of vegetation state, crop productivity and health status and photosynthetic capacity [52–57]. These variables of interest are also good proxies of the general health state of the crop and the use of remote sensing allows to estimate variations in these physical parameters at a relatively low cost compared to field measurements [55,58–60].

In recent times, field phenotyping and remote sensing are undergoing a process of convergence. Formally, field phenotyping refers to a quantitative description of a plant's phenotype devoid of spatial effects and remote sensing refers to the site-specific observation of vegetation by a remote device and the retrieval of its qualitative or quantitative properties. It is therefore clear that, traditionally, both disciplines concentrate on the interactions of plant growth with the surrounding environment with two different scopes: the first to generalise it, the second to explore site-specific interactions and describe spatially explicit traits [61].

The use of radiative transfer models, often rooted in artificial intelligence, to estimate plant traits from remotely sensed data can be considered the link between the generalisation and the spatialisation of data. The aim of radiative transfer models, which describe the radiation transfer and interactions of plant canopies based on physical laws, is to generalise empirical results and improve the robustness of vegetation parameter retrieval. Therefore, they are generally applicable in different situations [57,62]. When used in an inversion, the main bottleneck of radiative transfer models is the necessity to avoid ill-posed problems: to achieve this, prior information in order to reduce the number of possible variable retrieval options (combinations of canopy parameters) are required, also in order to improve the inversion accuracy [63–65]. Among radiative transfer models, the PROSAIL (PROSPECT (leaf optical properties spectra) + SAIL (Scattering from Arbitrarily Inclined Leaves) is widely used due to its simplicity, accuracy, and availability. Its robustness has been extensively tested through different sensors and platforms via ground, airborne, and spaceborne data sets [62].

The objective of this work was to identify whether UAV assisted image acquisition was a feasible means of detecting biostimulant treatment under water stress. The hypothesis tested here was whether retrieving LAI, LCC and CCC through PROSAIL inversion could efficiently detect the effect of a biostimulant (GB-based) treatment in open field on water stressed tomato and whether modelling this data dynamically through GAM could identify the windows of time where the biostimulant significantly impacted relevant traits. In order to achieve this, the PROSAIL was first validated through ground data, then inverted and applied to retrieve LAI, LCC and CCC and finally the dynamics of the effect on these parameters were investigated through GAM modelling. Additionally, the effect of the treatment on yield and quality parameters at harvest were tested.

2. Material and methods

2.1. Experimental site and set-up

Field experiments were conducted in the north-west of Italy, in Piacenza province, where the climate is continental with an average annual rainfall of 827 mm (1961–1990) and rainfall peaks in autumn and spring. The experiment was located in San Polo (44°59′14.6"N, 9°44′29.3"E) (Table 1).

The experimental layout (Fig. 1) is a randomised block design, with four blocks and single plot size of 75 m2 (1.5 × 10 × 5 m). The experiment was designed as a factorial combination of irrigation treatment (3 levels) and biostimulant treatment (3 levels). The levels of irrigation treatment were determined based on plant available water (PAW) ranges: i) 28.8<x<57.6, ii) 57.6<x<86.4 and iii) 86.4<x<144 in order to reach the respective thresholds of i) 25% PAW, ii)50% PAW and iii)100% PAW. The irrigation rate to maintain the three PAW levels was calculated based on the daily evapotranspiration (ET_c) reported in the web service IRRINET [66,67]. Concerning biostimulant treatment, the levels were three: untreated (control) (T0), treated twice at an interval of 2 weeks (T1), treated 3 times at intervals of 2 weeks (T2).

The experiment was conducted on tomato plants (*Lycopersicon esculentum, L.,* 3406 Heinz), which were transplanted on 17th of May 2020. Planting density and interrow spacing were the following: 5 m^{-2}, 0.2 m. Mineral fertilisation was carried out in two doses (200 kg N ha^{-1}) on 30/05/2020 and on 11/06/2020. Organic fertilisation was carried out on 4/06/2020 at a rate of 131 kg ha^{-1}. Fertilisation and weed/pest control have been performed using local agronomic recommendations. Drip irrigation was spaced as follows: 0.3 m (on row), 1.5 m (between rows), with a flow rate of 0.7 l h^{-1}. Irrigation was managed at the intervals

Table 1
Characteristics of the experimental location and weather data from 2020. Weather data from the closest climatic stations were retrieved with the web app of the Regional Environmental Protection Agency (www.arpae.it accessed on 20 December 2021), Dext3r (https://simc.arpae.it/dext3r/ accessed on 20 December 2021).

Parameter	
Location	San Polo, Piacenza
Latitude	44°59′14.6"N
Longitude	9°44′29.3"E
Elevation (m a.s.l.)	80
Texture class	silty clay loam
Yearly precipitation (mm)	520.8
Yearly maximum temperature (°C)	36.4
Yearly average temperature (°C)	15.5
Yearly minimum temperature (°C)	-5.6

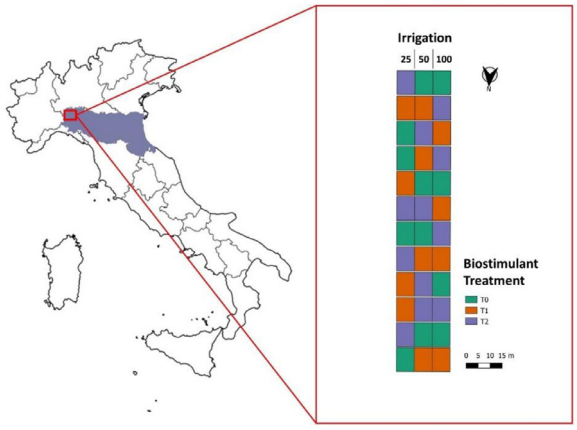

Fig. 1. Location of San Polo experimental site and overview of the experimental design and plots. Different colours represent the different biostimulant treatment levels. The three levels of irrigation are 25%, 50%, 100% PAW. Plots are representative of 15 m^2. Biostimulant treatments are indicated as follows: T0 = control treatment; T1 = treated twice; T2 = treated three times.

provided by the irrigation cooperative by fitting drip irrigation valves on every drip line and managing the quantity of water provided based on the duration of opening.

2.1.1. Biostimulant characteristics and treatment

The treatment with the biostimulant started on 23rd of June 2020 (37 days after transplant - DAT), at the start of flowering (Fig. 2).

Biostimulant was sprayed at a rate of 6 kg ha^{-1}, with a dilution of 300 l ha^{-1} to a total of 10 g/plant. Dose and dilution were chosen based on commercial use of the product (Vegetal B60®, ED&F MAN Liquid Products Italia, Bologna, Italy). Vegetal B60® is an organic product extracted exclusively from sugar beet without any added chemical additives. It contains 30% of GB and 5% of L–amino acids, 5% of total organic nitrogen, and 12% of organic carbon. The following treatments were carried out at two-week intervals: the second treatment was carried out on 52 DAT and the third at 65 DAT.

2.2. Field data collection

2.2.1. Model Parameter Acquisition

In situ leaf mass per unit leaf area (C_m) and leaf water per unit area (C_w) were calculated based on samples collected in an area of the field outside of the biostimulant trial (akin to an untreated plot). The leaves were separated from the stems and transferred to -18°C fridge. The leaf surface was determined by scanning the leaves, then the leaves were oven dried at 65°C. After drying, the leaves were weighted. The C_m (g cm^{-2}) and C_w (g cm^{-2}) were calculated as the ratio of the dry weight (C_m) or of the water weight (C_w) of the leaves and their surface. Destructive sampling from the biomass harvest was conducted over a total of 24 complete plants selected from 1 m^2 picketed plots over six samplings (Fig.2). Lastly, leaf area index was estimated using a ACCUPAR LP-80 PAR/LAI ceptometer (METER Group) on 5 dates across the season (18/06, 26/06, 10/07, 20/07, 06/08), The LP-80 measures photosynthetically active radiation (PAR, 400- to 700-nm). Jointly with C_m and C_w measurements, leaf samples for leaf chlorophyll content (LCC) determination were collected, immediately stored in ice, and transferred to a refrigerator (-20°C) for later analyses.

Chlorophyll was evaluated in two phases:

- Extraction (protocol adapted from [68]): samples were grinded in liquid nitrogen. Subsequently 0.1 g were weighted in 15 ml extraction tubes and 10 ml of absolute ethanol (99.8%) were added. Samples were homogenised by an Ultra-Turrax (Model T18) for 1 min. Thereafter samples were centrifuged at 4000 rpm at 4°C for 10 min. Concurrently, a subsample was put to dry at 105°C for 24 h in order to determine sample water content.
- Microplate Quantification: Microplate measurements were made by pipetting 250 µl of sample (or blank) in a 96-well white plate which was then read with a monochromator-based microplate reader (Synergy HT, BioTek, Winooski, USA) based on Warren [69]. The samples were read at 649 nm and 665 nm. Chlorophyll content was then calculated as follows [68]:

$$Chl_2\left(\mu g ml^{1}\right) = -5,2007 \times A_{649} + 13,5275 \times A_{665}$$

$$Chl_b\left(\mu g ml^{-1}\right) = 22,4327 \times A_{649} + \left(-7,0741 \times A_{665}\right)$$

2.2.2. Unmanned aerial vehicle multispectral image acquisition

The UAV used in the experiment was a four-rotator DJI Matrice 210 RTK (SZ DJI Technology Co., Shenzhen, Guangzhou, China) combined with a RTK (Real Time Kinematic) GPS positioning system. At each sampling event a UAV multispectral data acquisition was performed, in addition seven supplementary flight missions were carried out on each PS trial to increase the frequency of senescence tracking. Starting 27th May 2020, one multispectral UAV flight observation was conducted circa every week. Fourteen flights in total were performed across the season, five before the onset of treatments (Fig. 2). The drone was equipped with MicaSense RedEdge-Mx multispectral camera (MicaSense, Seattle, WA, USA). RedEdge-Mx camera can acquire 5 different spectral bands images: blue (475 nm centre, 32 nm bandwidth), green (560 nm centre, 27 nm bandwidth), red (668 nm centre, 14 nm bandwidth), red edge (717 nm centre, 12 nm bandwidth) and near-infrared (840 nm centre, 57 nm bandwidth). All the flights were performed between 11.00 and 15.00. The flight altitude above ground level (AGL) was 50 m. The forward overlap was set at 80% and lateral overlap was set at 75% of the images. The flight speed was set at 3 m/s. The ground sampling distance (GSD) was 2.78 cm. The flight was performed in automatic mode with waypoints routes as the presence of a GPS navigation system enables a more accurate image acquisition. The DJI Pilot software (SZ DJI Technology Co., Shenzhen, Guangzhou, China) was used for flight planning and automatic mission control. For the radiometric calibration of the images, the reflectance of a spectral panel (MicaSense, Seattle, WA, USA) with reflectance values provided by MicaSense, was captured before each flight. In addition, a light sensor that automatically adjusts the readings to ambient light was mounted at the top of the UAV to minimise error during image capture. The radiometric calibration, image mosaicking and orthomosaic generation were done using the Pix4D mapper (Pix4D, S.A., Lausanne, Switzerland). To extract the spectral information of each experimental plot, the polygons of the experimental design were drafted in AutoCAD (Autodesk, San Rafael, California, USA) and georeferenced based on the UAV multispectral images by using QGIS software (QGIS Development Team, 2021).

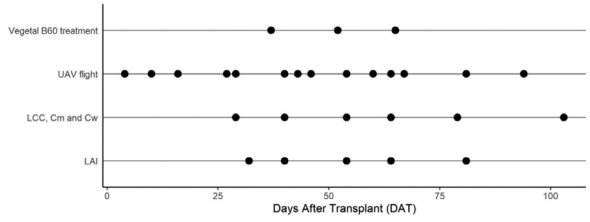

Fig. 2. Vegetal B60 treatment, UAV flight, sampling (LCC, Cm and Cw) and leaf area index (LAI) ground measurements seasonal calendar.

2.3. Final yield and post-harvest analyses

The final harvest was carried out between 25th of August 2020 and 28th of August 2020. The same theses were harvested across blocks to

minimise between-block variability. The harvested area was 1 m^2 repeated three times for each plot, for a total of 3 m^2 per plot. The harvest was divided between the biomass portion (leaves and stems) and the fruit portion, further classified in green, rotten and red fraction. A subsample for biomass and red fruits was oven dried at 105°C to determine their dry matter (DM) content.

Total soluble solids (TSS) and pH were measured on circa 200 g of homogenised fresh fruit subsamples from the total red fruits harvested. Every measurement was repeated thrice. TSS were measured via a digital refractometer (RX-5000 ATAGO, U.S.A., Bellevue, WA). The pH of the samples was measured via a digital pH meter (HI 5522, HANNA, USA).

2.4. Radiative tranfer model: PROSAIL

Leaf area index (LAI), leaf chlorophyll content (LCC) and canopy chlorophyll content (CCC) were retrieved though the inversion of the PROSAIL model [62]. In PROSAIL data are derived from combining the PROSPECT leaf optical properties model and the SAIL canopy bidirectional reflectance model. The PROSPECT (Feret et al., 2008) model simulates the leaf reflectance and transmittance in the range from 400 to 2500 nm with four parameters: leaf structure parameter (N), leaf chlorophyll content (LCC), leaf dry matter content (C_m), and leaf equivalent water thickness (C_w).

The SAIL model is a radiative transfer model used to simulate the bidirectional reflectance of a canopy. The PROSAIL requires fourteen parameters in order to run: N, LCC, C_w, C_m, LAI, hot-spot parameter (hot spot), observer zenith angle (tto), sun zenith angle (tts), relative azimuth angle (psi), and average leaf angle (ALA). The PROSAIL inputs (parameter combinations) and outputs (spectral reflectance) were used to generate a database. In the database generation, 48,600 parameter combinations were generated following the ranges (minimum and maximum) and the step of the parameters summarised in Table 2. The ranges were optimised based on data collected in the field (see chapter 2.2): this is an efficient way of solving the ill-posed problem as suggested by Meroni et al. [70]. The spectral reflectance simulated (outputs) were resampled based on UAV cameras characteristics.

2.5. Gaussian process regression (GPR) based PROSAIL inversion

Rooted in large dataset modelling, machine learning (ML) algorithms enable more accurate data mining by learning from training data to model, classify, and predict the variables in the whole datasets [71].

Gaussian process regression (GPR) is a vigorous, non-parametric Bayesian method used for solving regression problems and unknown modelling functions [72,73]. Its main feature is capturing the different relationships between inputs and output variables by applying a hypothetically infinite number of parameters and allowing the dataset to determine the level of complexity via Bayesian inference [74]. The parametrization of the Gaussian process is made using a kernel, the choice of which is flexible. Moreover, it is possible to combine the different kernels to perform the regression [72]. In this study, GPR radial basis function kernel was used to invert the PROSAIL database to retrieve LAI, LCC and CCC data by using the "caret" package [75]. GPR was used as part of a combination between a RTM and a ML algorithm in order to retrieve crop biophysical traits. This combinations are commonly referred to as hybrid methods and they allow replacing the field measurements needed to train non-parametric models with RTM models (such as PROSAIL) input variables [76]. The GPR algorithm was chosen based on the aforementioned characteristics and based on the works of Verrelst et al. [77]. GPR was trained with the 5 spectral reflectance simulated by PROSAIL model and resampled thereafter. The structural hyperparameters of the GPR models were optimized by grid-searching method using cross-validation. These retrieved biophysical traits were proxies to discriminate between irrigation and biostimulant treatments and their combination.

The coefficient of determination (R^2) (1) and Root Mean Square Error as such (RMSE) (2) and normalised against the mean (nRMSE) (3) were used to quantify the amount of variation explained, as well as the accuracy, of those relationships. The performance of the model was estimated by comparing differences in the R^2 and RMSE. The closer R^2 scored to 1 and the lower RMSE scored, the higher were the precision and accuracy of the inversion, and vice-versa.

$$R^2 = \frac{\left(\sum_{i=1}^{n}\left(p_i-\bar{p}_i\right)\left(f_i-\bar{f}_i\right)\right)^2}{\sum_{i=1}^{n}\left(p_i-\bar{p}_i\right)^2 \sum_{i=1}^{n}\left(f_i-\bar{f}_i\right)^2} \quad (1)$$

$$RMSE = \sqrt{\frac{1}{n}\sum_{i=1}^{n}\left(p-f_i\right)^2} \quad (2)$$

$$nRMSE\ (\%) = \frac{RMSE}{\bar{p}_i}\ 100 \quad (3)$$

where n (i = 1, 2, …, n) is the number of samples used to test ML model, p_i is the observed parameter (LAI, LCC or CCC), $\bar{p}_i$ is the corresponding mean value, f_i is the predicted parameter and $\bar{f}_i$ is the corresponding mean value.

2.6. Statistical analyses

Statistical analyses were performed using RStudio, R version 4.0.4 (R Core Team, 2020).

2.6.1. ANOVA

Crop yield data (both fresh and dry matter) were analysed through two-way ANOVA to determine the significance of irrigation and biostimulant treatments and their interaction with the following model: lm(yield ~ irrigation × biostimulant treatment) followed by a pairwise comparison with the formula: emmeans(model, specs = irrigation × biostimulant treatment, adjust = 'sidak'), with the "emmeans" v.1.5.4 R package.

2.6.2. Generalised additive models (GAM) for phenotyping tomato water stress dynamic

To phenotype the dynamics of LAI, CCC and LCC and identify differences among biostimulant and irrigation treatments, statistical analysis

Table 2
LUT generation parameters ranges.

Parameter		Abbreviation	Unit	Values
Leaf	Structure parameter	N	Unitless	1.25
	Chlorophyll content	LCC	μg cm^{-2}	30 – 72 (step = 3)
	Equivalent water thickness	C_w	g cm^{-2}	0.022 – 0.028 (step = 0.003)
	Dry matter content	C_m	g cm^{-2}	0.003 – 0.004 (step = 0.0005)
Canopy	Leaf area index	LAI	m^2 m^{-2}	0.1 – 6 (step = 0.3)
	Average leaf angle	ALA	deg	50 – 70 (step = 10)
	Hotspot parameter	hot	m m^{-1}	0.1
	Sun zenith angle	tts	deg	20 – 30 (step = 5)
	Observer zenith angle	tto	deg	10
	Relative azimuth angle	psi	deg	190 – 195

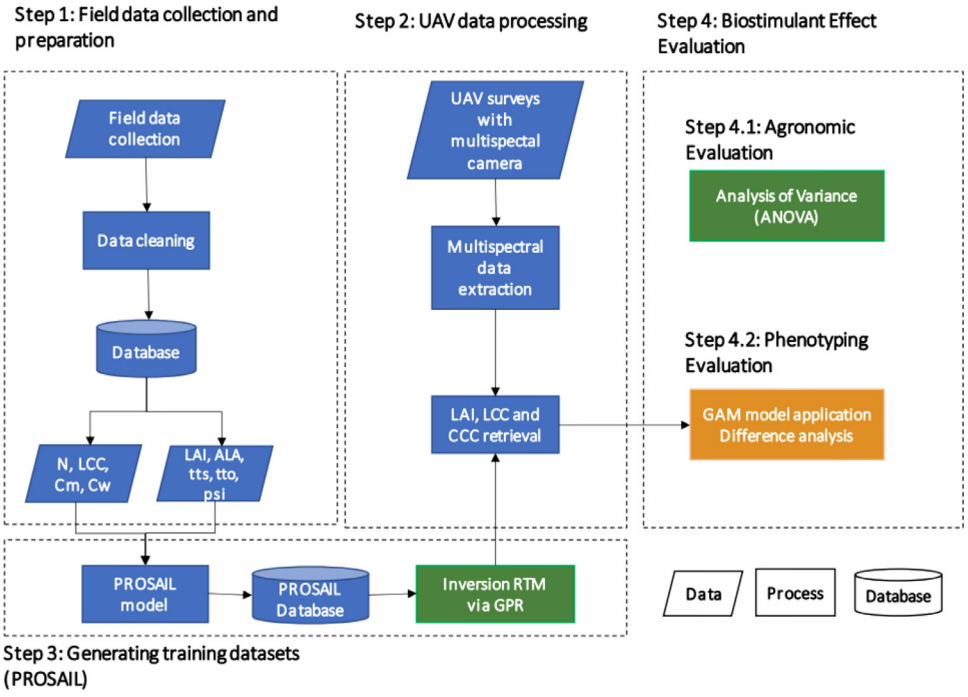

Fig. 3. Overview of the objectives of this study and the implemented workflow.

of the traits time series was carried out via a generalised additive model (GAM). GAM are non-parametric regression models, which allow the integration of non-parametric smoothing functions and non-linear fitting of the variables. GAM models were fitted in R package "*itsadug*" (van Rij et al., 2020). The fitted model used biostimulant treatment and irrigation treatment as fixed factors and a smooth for DAT, while considering the block as a random error.

2.7. Biostimulant effect evaluation workflow

Agronomic (fresh fruit yield, fruit dry matter) and model parameter data (C_m, LCC, LAI) were collected in the field. Agronomic data output was then analysed through two-way analysis of variance (ANOVA, detailed in section 2.5.1) while model parameter data were first used to narrow the range of the database, and then to validate the PROSAIL model. The PROSAIL database generated was then used to train the GPR model to retrieve leaf area index (LAI), leaf chlorophyll content (LCC) and canopy chlorophyll content (CCC) of the crop from multispectral images. Finally, the data thus generated were analysed through generalised additive modelling (GAM, described in further detail in section 2.5.2) in order to evaluate the effect of the biostimulant application. The process is summarised in Fig. 3.

3. Results

3.1. Crop yield and quality parameters

Red fruit yield, both determined as fresh weight (Fig. 4a) and dry weight (Fig. 4b), was statistically affected by irrigation treatments but not by the biostimulant treatments.

5The analysis of total soluble solids (TSS) resulted in a significant difference in the sugar content among the two lower irrigation treatments and the control (100% PAW) treatment (Fig. 4c). The two lower-level treatments (25 and 50% PAW) did not display any significant difference among them. Also in this case the effect of the biostimulant treatment, was not significant.

3.2. PROSAIL validation

The accuracy of LAI, LCC and CCC retrieved from the inversion of PROSAIL was evaluated against the independent dataset obtained from

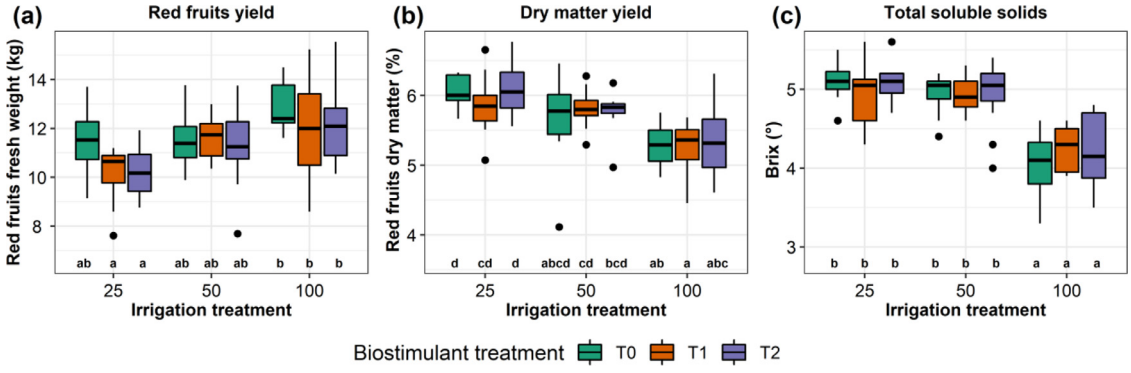

Fig. 4. Agronomic response of tomato in terms of red fruit yield (kg) (a), dry matter yield (%) (b) and total soluble solids (TSS) (Brix°) (c) to three levels of irrigation (25%, 50%, 100% PAW). Data are representative of 12 m^2 per each combination of treatment. Biostimulant treatments are indicated as follows: T0 = control treatment; T1 = treated twice; T2 = treated three times. Different letters (a,b,c,d) at the bottom of the graphs indicate statistically significant differences according to Sidak-test.

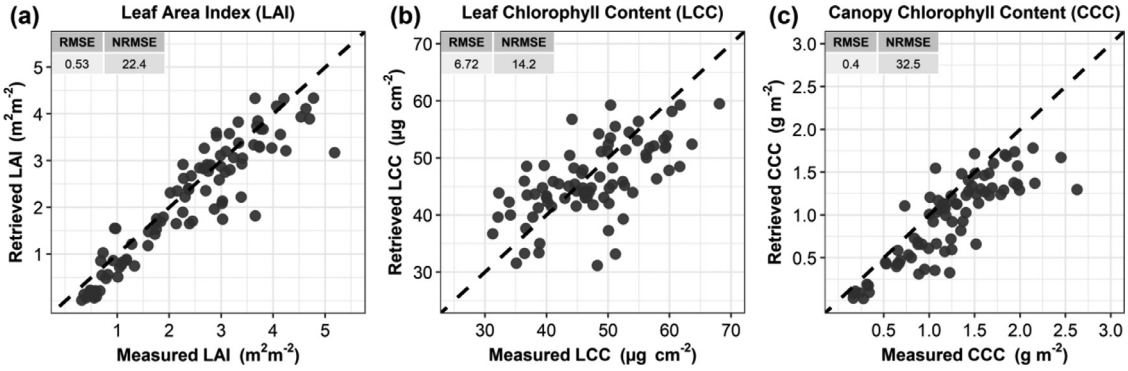

Fig. 5. Comparison between the in-situ measurements and the retrieved LAI (a), LCC (b), CCC (c).

Table 3
Characteristics of models for LAI and CCC. Dev. Expl. (%) = deviance explained.

Model	R^2	Dev. Expl (%)
LAI	0.844	85.1
LCC	0.562	58.1
CCC	0.840	84.7

in-situ measurements. The RMSE value for LAI estimates was 0.53 m^2 m^{-2} (Fig. 5a). The RMSE value for LCC scored 6.72 µg cm^{-2} (Fig. 5b). Finally, the RMSE value for CCC (Fig. 5c) was 0.4 g m^{-2}. Nevertheless, in terms of nRMSE score, the best results were obtained for LCC (14.2 %) when compared to LAI (22.4 %) and CCC (32.5 %) (Fig. 5).

3.3. GAM analysis of GPR inversion for LAI, LCC and CCC retrieval

After the PROSAIL model validation, LAI, LCC and CCC data were examined through generalised additive modelling (GAM) to evaluate the fitness of the combination of these techniques for biostimulant testing. GAM analysis was used to model dynamic seasonal data in order to evaluate the changes induced by biostimulant treatment, irrigation treatment and their interaction on the biophysical traits. GAMs are non-linear regression models, which are characterised by a sum of smooth functions.

The GAM model implemented had the following structure: gam (CCC ~ Biostimulant Treatment * Irrigation Treatment + s(DAT, by = Irrigation Treatment, k = 5) + s(DAT, by = Treat, k = 5) + s(Block, bs = "random error").

Where s stands for single effect smooths, k is the number of kernels, namely the dimension of the basis used to represent the smooth term, and bs indicates the penalised smoothing basis, in this case the random error. K was choosen based on the indications of Wood [78]. The R^2 and explained deviance of LAI, LCC and CCC model scores showed that the models could explain large amounts of variance (Table 3).

3.3.1. Irrigation treatments analysed via GAM

Irrigation treatments were efficiently discriminated across the season via GAM analysis.

Concerning LAI, the comparison between irrigation levels highlighted a statistically significant difference between the 100% versus 50% and the 100% versus 25% PAW (Fig. 6A).

The significant difference between 100% and 50% started on 32 DAT and ended on 48 DAT, while the significant difference between 100% and 25% treatments started on 30 DAT until 81 DAT. In both cases 100% PAW treatment performed better than the other two theses, ranging from +0.1 to +0.45 in estimated difference. LCC comparison between irrigation levels highlighted no statistically significant difference among treatments (Fig. 6B). Concerning CCC, the comparison between irrigation levels highlighted a statistically significant difference among the 100% versus 50% and the 100% versus 25% PAW (Fig. 6C). The significance of the 100% versus 25% treatments started on DAT 31 until 66 DAT, while the significant difference between 100% and 50% started on 33 DAT and ended on 44 DAT. In both cases 100% PAW treatment performed better than the other two theses in a range from +0.05 to +0.25 in estimated difference.

3.3.2. Biostimulant treatments analysed via GAM

Biostimulant treatment was evaluated with the same statistical approach as irrigation treatment. Concerning LAI (Fig. 7A), the comparison between biostimulant treatments resulted in a statistically significant difference among the control treatment (T0) versus T2 (treated twice) treatment early in the season (27 DAT) until 53 DAT: the highest difference was detected around 25 DAT (-0.2), where T2 was higher.

Nevertheless, when this data was matched with the treatment calendar, that is the DAT at which the biostimulant treatments were performed (Table 2), the significant difference between T0 and T2 started before the first biostimulant treatment was applied (37 DAT).

Concerning LCC (Fig. 7B) and CCC (Fig. 7C), the comparison between biostimulant treatments across the season resulted in no statistically significant difference.

3.3.3. Irrigation and biostimulant treatments analysed via GAM

When displayed as combination of irrigation and biostimulant treatment, no significant difference could be detected. The comparisons were carried out for each irrigation treatment across biostimulant treatments (e.g. treatment 1 versus treatment 2 at 25% PAW) for LAI, LCC and CCC. Significant differences were detected only between the control (T0) and T1 (twice) and between T0 (control) and T2 (thrice) under 25% PAW irrigation. As for biostimulant treatment alone, when this data was matched with the treatment calendar (that is the DAT at which the biostimulant treatments were performed (Table 2)) the significant differences were shown to start before the first biostimulant treatment was applied (37 DAT).

4. Discussion

Spectral data from UAV are commonly used to monitor crop stress response [24–26]. Nevertheless, remote sensing applied to agriculture still faces a challenge: understanding how the collected data can be effectively utilised to characterise biophysical properties of the crop canopy [79].

With the support of big data analysis, acquired spectral data enable the estimation of crop biophysical properties. This is particularly interesting in contexts where experimental replicates are limited (because of practical or experimental design related constraints and costs) while the main goal would be still to generalise experimental findings to the field scale and above. In this context, the PROSAIL model has been widely used to assess crop traits, such as the LCC, C_w, C_m and LAI [62]. In this

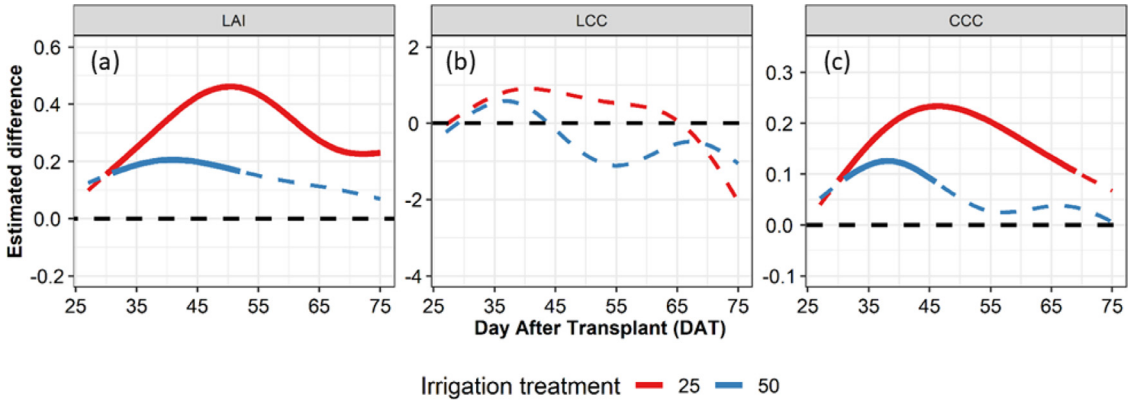

Fig. 6. Difference between irrigation treatments for the three parameters (LAI, LCC, CCC) analysed via GAM. The dashed horizontal baseline represents treatment 100% PAW. When lines are full, the difference between that treatment and 100% PAW is significant (95% c.i.). Conversely, when lines are dashed the difference is not significant.

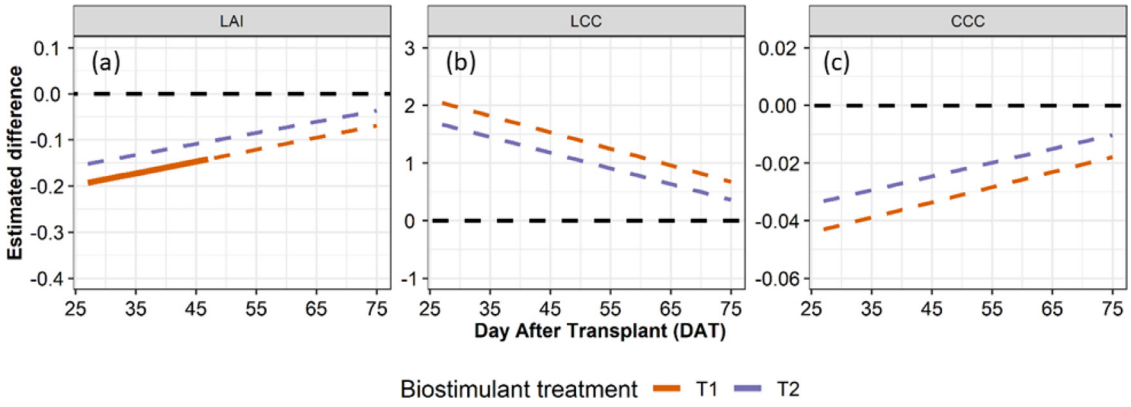

Fig. 7. Difference between biostimulant treatments for the three parameters (LAI, LCC, CCC) analysed via GAM. The dashed horizontal baseline represents control treatment (T0). When lines are full, the difference between that treatment and T0 is significant (95% c.i.). Conversely, when lines are dashed the difference is not significant. T1 = treated twice, T2 = treated three times.

sense, multiple approaches are being investigated: among these, machine learning (ML)-assisted radiative transfer model inversion is gaining importance as a means to enhance the robustness and transferability of biophysical traits retrieval.

4.1. Crop yield

Water deficiency directly affects primary metabolism [80], resulting in variations in crop yield and dry matter (DM) content. At the same time, in tomato, water stress increases TSS content [81]. This was confirmed in the present experiment: red fruits yield was lower at the lowest irrigation treatment (25% PAW) than at the highest one (100% PAW). The same result was found for DM, despite it displaying a more scattered behaviour compared to fresh yield.

4.2. PROSAIL validation

While no significant difference could be detected for LCC and CCC related to biostimulant treatments, these data are in agreement with those retrieved from the PROSAIL inversion, corroborating its reliability. PROSAIL validation was carried out on multispectral data and, when considering LAI, yielded RMSE (0.53 m^2 m^{-2}) results comparable to validations carried out on hyperspectral data based on smaller datasets [44] or achieved a better accuracy [42]. On the other hand, relationships between simulated and measured LCC indicated a better relationship in terms of nRMSE, compared to LAI and CCC, between sampled and simulated data. Moreover, the RMSE value (6.72 μg cm^{-2}) obtained for LCC was consistent with those found by Botha and colleagues [82] on potato and the multispectral data retrieved by Wan and colleagues [83] for rice and rapeseed (5.40 μg cm^{-2}), but considerably better than what found by Li and colleagues, (2015) for hyperspectral-base retrievals of LCC on winter wheat (13.36 and 9.35 μg cm^{-2}). CCC retrieval performance in terms of RMSE (0.4 g m^{-2}) could probably be due to the strong influence of LAI in the relation: CCC represents the canopy-integrated chlorophyll content (LAI × leaf chlorophyll content), which is strongly influenced by the variability in LAI, especially when chlorophyll content is stable [84]. This was also modelled by generalised additive model (GAM) graphs, which displayed trends very similar to LAI GAM graphs. On the other hand, PROSAIL model is most appropriate for homogeneous canopies: the turbid medium assumptions at its core negatively influence its capability to model non-uniform canopies such as crop-row canopies [85]. This represents a bottleneck that hampers the efficient implementation of PROSAIL on processing tomato: the nRMSE for CCC retrieval was 32.5 %, the highest among the three parameters, probably due to the characteristics of processing tomato canopy. This is further confirmed by the findings of Roojen and colleagues (2018), whose results on nadir LAI and LCC, were consistent with the findings of this study while performed much better when considering multi-angular simulations. Thanks to the sensitivity of multi-angular measurements to vegetation structure, these simulations take into account information on the structural properties of the canopy [86,87].

4.3. GAM analysis of GPR inversion for LAI, LCC and CCC retrieval

LAI, LCC and CCC were later analysed via GAM. The influence of irrigation and biostimulant treatments were evaluated both separately

and jointly. When considering irrigation alone, the comparison between irrigation levels highlighted a statistically significant difference between the 100% versus 50% and the 100% versus 25% PAW. LCC, in turn displayed no significant difference between the two deficit irrigation treatments and the control treatment.

In terms of biostimulant action evaluation alone, the effects highlighted via GAM analysis were later matched with the treatment calendar, that is the DAT at which the biostimulant treatments were performed: the significant difference between T0 and T2 started before the first biostimulant treatment was applied (37 DAT). Moreover, the magnitude of the effect (-0.2 maximum) for LAI was negligible when compared to the RMSE error from the PROSAIL validation (0.53 m^2 m^{-2}). These two aspects do not support the validity of the differences retrieved via GAM.

When both parameters (irrigation x biostimulant treatment) were included in the pairwise comparisons for each irrigation level, none of the biophysical traits displayed a significant difference.

4.4. Biostimulant effect: overarching considerations

The properties of glycinebetaine [6,10,12,16,17,21] indicate the possibility that GB-based biostimulants stabilise chlorophyll content across the season when the crop is undergoing water stress. At the same time, the maintenance of photosynthetic activity related to the protection of photosystems would indicate the possibility of achieving a higher LAI across the season compared to the untreated stressed crop. However, the present research was not able to observe any significant result of GB treatment on LCC and CCC and the effects observed on LAI were inconclusive. Generalised additive models were chosen in order better analyse the dynamic time-series dataset. The goal of the GAM analysis was to discriminate the effect of treatments (i.e., irrigation and biostimulant application) on the patterns (i.e., wiggliness) of LAI, LCC and CCC. Despite the successful application of GAM to model dynamic data on biostimulant action in a previous experiment on processing tomato in greenhouse [88], the results from the current experiment did not enable an effective detection and modelling of the biostimulant effect. In the comprehensive review by Wozniak and colleagues [89] on the effects of biostimulants at whole-plant level amino acid-based and protein hydrolysates as a class were reported to increase the production of a limited number of crops [90–92], while at the same time reporting no influence on others [93,94]. This leads to think that the effects of biostimulant application in the field could be much more difficult to pin down than those of other products (such as fertilisers or pesticides) or even inconsistent, especially when considering the work of Mäkelä and colleagues [95] who, contrary to this work, found that exogenous glycinebetaine applied to salt or heat stressed tomato crops during flowering resulted in an increase in fruit yield up to 39%.

On-field research on biostimulant effects has been on the rise in the last few years, but the results on most parameters are elusive: this is further confirmed, for example, by the work from Francesca and colleagues [96], who tested the efficacy of a biostimulant treatment on water deficient tomato crops in open field, only found significant effects on stomatal conductance and pollen viability.

5. Conclusions

In the framework of biostimulant testing, this was the first attempt at utilising biophysical traits retrieved from PROSAIL inversion in order to quantify the effect of a biostimulant. The validation of the model was carried out with a positive outcome regarding accuracy. However, the internal variability per plot of the retrieved biophysical traits was high. This, jointly with the uncertainty surrounding biostimulant testing and the magnitude of biostimulant effects, corroborated by the absence of results regarding biostimulant effect on yield and DM, leads to hypothesise that the bottleneck does not lie at the PROSAIL inversion stage, but is rather linked to the biostimulant effect itself. The PROSAIL inversion enabled the efficient retrieval of LAI and LCC at rates comparable to those in literature, while performing worse than literature findings only for CCC, probably due to the characteristics of tomato canopy.

Declaration of Competing Interest

The authors declare no competing interest.

CRediT authorship contribution statement

Giulia Antonucci: Conceptualization, Data curation, Methodology, Investigation, Formal analysis, Writing – original draft. **Giorgio Impollonia:** Conceptualization, Data curation, Methodology, Investigation, Software, Writing – review & editing. **Michele Croci:** Conceptualization, Data curation, Investigation, Software, Writing – review & editing. **Eleonora Potenza:** Investigation, Data curation. **Andrea Marcone:** Investigation. **Stefano Amaducci:** Conceptualization, Funding acquisition, Project administration, Supervision, Writing – review & editing.

Acknowledgments

The authors gratefully acknowledge financial support from ED&F Man Liquid products ITALIA SRL (Bologna, Italy).

References

[1] W.G. Buma, S.I. Lee, Multispectral Image-Based Estimation of Drought Patterns and Intensity around Lake Chad, Africa, Remote Sensing 11 (21) (2019) 2534, doi:10.3390/rs11212534.
[2] D. Del Buono, Can biostimulants be used to mitigate the effect of anthropogenic climate change on agriculture? It is time to respond, Sci. Total Environ. 751 (2020) 141763, doi:10.1016/j.scitotenv.2020.141763.
[3] A. Michaletti, M.R. Naghavi, M. Toorchi, L. Zolla, S. Rinalducci, Metabolomics and proteomics reveal drought-stress responses of leaf tissues from spring-wheat, Scientific Reports 8 (1) (2018) 5710, doi:10.1038/s41598-018-24012-y.
[4] H. Medrano, J.M. Escalona, J. Bota, J. Giulias, J. Flexas, Regulation of Photosynthesis of C3 Plants in Response to Progressive Drought: Stomatal Conductance as a Reference Parameter, Annals of Botany 89 (7) (2002) 895–905, doi:10.1093/aob/mcf079.
[5] G.C. Papageorgiou, Y. Fujimura, N. Murata, Protection of the oxygen-evolving photosystem II complex by glycinebetaine, Biochimica et Biophysica Acta (BBA) - Bioenergetics 1057 (3) (1991) 361–366, doi:10.1016/s0005-2728(05)80148-3.
[6] G.C. Papageorgiou, N. Murata, The unusually strong stabilizing effects of glycine betaine on the structure and function of the oxygen-evolving Photosystem II complex, Photosynthesis Research 44 (3) (1995) 243–252, doi:10.1007/bf00048597.
[7] S. Mbarki, O. Sytar, A. Cerda, M. Zivcak, A. Rastogi, X. He, A. Zoghlami, C. Abdelly, M. Brestic, Strategies to mitigate the salt stress effects on photosynthetic apparatus and productivity of crop plants, in: Salinity responses and tolerance in plants, 1, Springer, Berlin, 2018, pp. 85–136.
[8] X. Tang, X. Mu, H. Shao, H. Wang, M. Brestic, Global plant-responding mechanisms to salt stress: physiological and molecular levels and implications in biotechnology, Critical Reviews in Biotechnology 35 (4) (2014) 425–437, doi:10.3109/07388551.2014.889080.
[9] F. Tian, W. Wang, C. Liang, X. Wang, G. Wang, W. Wang, Overaccumulation of glycine betaine makes the function of the thylakoid membrane better in wheat under salt stress, The Crop Journal 5 (1) (2017) 73–82, doi:10.1016/j.cj.2016.05.008.
[10] X. Yang, C. Lu, Photosynthesis is improved by exogenous glycinebetaine in salt-stressed maize plants, Physiologia Plantarum 124 (3) (2005) 343–352, doi:10.1111/j.1399-3054.2005.00518.x.
[11] R. Quan, M. Shang, H. Zhang, Y. Zhao, J. Zhang, Improved chilling tolerance by transformation with betA gene for the enhancement of glycinebetaine synthesis in maize, Plant Science 166 (1) (2004) 141–149, doi:10.1016/j.plantsci.2003.08.018.
[12] S.I. Allakhverdiev, H. Hayashi, Y. Nishiyama, A.G. Ivanov, J.A. Aliev, V.V. Klimov, N. Murata, R. Carpentier, Glycinebetaine protects the D1/D2/Cytb559 complex of photosystem II against photo-induced and heat-induced inactivation, Journal of Plant Physiology 160 (1) (2003) 41–49, doi:10.1078/0176-1617-00845.
[13] X. Yang, X. Wen, H. Gong, Q. Lu, Z. Yang, Y. Tang, Z. Liang, C. Lu, Genetic engineering of the biosynthesis of glycinebetaine enhances thermotolerance of photosystem II in tobacco plants, Planta 225 (3) (2006) 719–733, doi:10.1007/s00425-006-0380-3.
[14] F. Razavi, R. Mahmoudi, V. Rabiei, M.S. Aghdam, A. Soleimani, Glycine betaine treatment attenuates chilling injury and maintains nutritional quality of hawthorn fruit during storage at low temperature, Scientia Horticulturae 233 (2018) 188–194, doi:10.1016/j.scienta.2018.01.053.
[15] L. Wang, T. Shan, B. Xie, C. Ling, S. Shao, P. Jin, Y. Zheng, Glycine betaine reduces chilling injury in peach fruit by enhancing phenolic and sugar metabolisms, Food Chemistry 272 (2019) 530–538, doi:10.1016/j.foodchem.2018.08.085.
[16] Q.Q. Ma, W. Wang, Y.H. Li, D.Q. Li, Q. Zou, Alleviation of photoinhibition in drought-stressed wheat (Triticum aestivum) by foliar-applied glycinebetaine, Journal of Plant Physiology 163 (2) (2006) 165–175, doi:10.1016/j.jplph.2005.04.023.

[17] M. Ashraf, M. Foolad, Roles of glycine betaine and proline in improving plant abiotic stress resistance, Environmental and Experimental Botany 59 (2) (2007) 206–216, doi:10.1016/j.envexpbot.2005.12.006.
[18] T.H. Chen, N. Murata, Glycinebetaine protects plants against abiotic stress: mechanisms and biotechnological applications, Plant, Cell and Environment 34 (1) (2010) 1–20, doi:10.1111/j.1365-3040.2010.02232.x.
[19] J. Gorham, Betaines in higher plants – biosynthesis and role in stress metabolism, in: R.M. Wallsgroves (Ed.), Amino Acids and Their Derivatives in Higher Plants, Cambridge University Press, Cambridge, 1995, pp. 171–203.
[20] S. Huang, T. Zuo, W. Ni, Important roles of glycinebetaine in stabilizing the structure and function of the photosystem II complex under abiotic stresses, Planta 251 (2) (2020) x, doi:10.1007/s00425-019-03330-z.
[21] A. Sakamoto, N. Murata, The role of glycine betaine in the protection of plants from stress: clues from transgenic plants, Plant, Cell and Environment 25 (2) (2002) 163–171, doi:10.1046/j.0016-8025.2001.00790.x.
[22] T.R. Fleming, C.C. Fleming, C.C.B. Levy, C. Repiso, F. Hennequart, J.B. Nolasco, F. Liu, Biostimulants enhance growth and drought tolerance inArabidopsis thalianaand exhibit chemical priming action, Annals of Applied Biology 174 (2) (2019) 153–165, doi:10.1111/aab.12482.
[23] Y. Rouphael, L. Spíchal, K. Panzarová, R. Casa, G. Colla, High-Throughput Plant Phenotyping for Developing Novel Biostimulants: From Lab to Field or From Field to Lab? Frontiers in Plant Science 9 (2018), doi:10.3389/fpls.2018.01197.
[24] J. Barbedo, A Review on the Use of Unmanned Aerial Vehicles and Imaging Sensors for Monitoring and Assessing Plant Stresses, Drones 3 (2) (2019) 40, doi:10.3390/drones3020040.
[25] C. Xie, C. Yang, A review on plant high-throughput phenotyping traits using UAV-based sensors, Computers and Electronics in Agriculture 178 (2020) 105731, doi:10.1016/j.compag.2020.105731.
[26] A. Galieni, N. D'Ascenzo, F. Stagnari, G. Pagnani, Q. Xie, M. Pisante, Past and Future of Plant Stress Detection: An Overview From Remote Sensing to Positron Emission Tomography, Frontiers in Plant Science 11 (2021), doi:10.3389/fpls.2020.609155.
[27] J. Yue, G. Yang, C. Li, Z. Li, Y. Wang, H. Feng, B. Xu, Estimation of Winter Wheat Above-Ground Biomass Using Unmanned Aerial Vehicle-Based Snapshot Hyperspectral Sensor and Crop Height Improved Models, Remote Sensing 9 (7) (2017) 708, doi:10.3390/rs9070708.
[28] H. Zheng, T. Cheng, D. Li, Y. Xia, Y. Tian, W. Cao, et al., Combining Unmanned Aerial Vehicle (UAV)-Based Multispectral Imagery and Ground-Based Hyperspectral Data for Plant Nitrogen Concentration Estimation in Rice, Front. Plant Sci. 9 (2018) 936, doi:10.3389/fpls.2018.00936.
[29] S. Heinemann, B. Siegmann, F. Thonfeld, J.M. Martín, U. Rascher, Land Surface Temperature Retrieval for Agricultural Areas Using a Novel UAV Platform Equipped with a Thermal Infrared and Multispectral Sensor, Remote Sens. 12 (2020) 1075, doi:10.3390/rs12071075.
[30] L. Qiao, D. Gao, J. Zhang, M. Li, J. Ma, Dynamic Influence Elimination and Chlorophyll Content Diagnosis of Maize Using UAV Spectral Imagery, Remote Sens 12 (2020) 2650, doi:10.3390/rs12162650.
[31] W.H. Maes, K. Steppe, Estimating evapotranspiration and drought stress with ground-based thermal remote sensing in agriculture: a review, Journal of Experimental Botany 63 (13) (2012) 4671–4712, doi:10.1093/jxb/ers165.
[32] W.H. Maes, K. Steppe, Perspectives for Remote Sensing with Unmanned Aerial Vehicles in Precision Agriculture, Trends in Plant Science 24 (2) (2019) 152–164, doi:10.1016/j.tplants.2018.11.007.
[33] C. Zhang, J.M. Kovacs, The application of small unmanned aerial systems for precision agriculture: a review, Precision Agriculture 13 (6) (2012) 693–712, doi:10.1007/s11119-012-9274-5.
[34] H. Tao, H. Feng, L. Xu, M. Miao, H. Long, J. Yue, Z. Li, G. Yang, X. Yang, L. Fan, Estimation of Crop Growth Parameters Using UAV-Based Hyperspectral Remote Sensing Data, Sensors 20 (5) (2020) 1296, doi:10.3390/s20051296.
[35] G. Impollonia, M. Croci, E. Martani, A. Ferrarini, J. Kam, L.M. Trindade, J. Clifton-Brown, S. Amaducci, Moisture content estimation and senescence phenotyping of novel Miscanthus hybrids combining UAV based remote sensing and machine learning, GCB Bioenergy (2022), doi:10.1111/gcbb.12930.
[36] M. Domingues Franceschini, H. Bartholomeus, D. van Apeldoorn, J. Suomalainen, L. Kooistra, Intercomparison of Unmanned Aerial Vehicle and Ground-Based Narrow Band Spectrometers Applied to Crop Trait Monitoring in Organic Potato Production, Sensors 17 (6) (2017) 1428, doi:10.3390/s17061428.
[37] S. Jay, F. Maupas, R. Bendoula, N. Gorretta, Retrieving LAI, chlorophyll and nitrogen contents in sugar beet crops from multi-angular optical remote sensing: Comparison of vegetation indices and PROSAIL inversion for field phenotyping, Field Crops Research 210 (2017) 33–46, doi:10.1016/j.fcr.2017.05.005.
[38] C. Cilia, C. Panigada, M. Rossini, M. Meroni, L. Busetto, S. Amaducci, M. Boschetti, V. Picchi, R. Colombo, Nitrogen Status Assessment for Variable Rate Fertilization in Maize through Hyperspectral Imagery, Remote Sensing 6 (7) (2014) 6549–6565, doi:10.3390/rs6076549.
[39] J.P. Goffart, M. Olivier, M. Frankinet, Potato Crop Nitrogen Status Assessment to Improve N Fertilization Management and Efficiency: Past–Present–Future, Potato Research 51 (3–4) (2008) 355–383, doi:10.1007/s11540-008-9118-x.
[40] P.P. Roosjen, B. Brede, J.M. Suomalainen, H.M. Bartholomeus, L. Kooistra, J.G. Clevers, Improved estimation of leaf area index and leaf chlorophyll content of a potato crop using multi-angle spectral data – potential of unmanned aerial vehicle imagery, International Journal of Applied Earth Observation and Geoinformation 66 (2018) 14–26, doi:10.1016/j.jag.2017.10.012.
[41] M. Kanning, I. Kühling, D. Trautz, T. Jarmer, High-Resolution UAV-Based Hyperspectral Imagery for LAI and Chlorophyll Estimations from Wheat for Yield Prediction, Remote Sensing 10 (12) (2018) 2000, doi:10.3390/rs10122000.
[42] S.B. Duan, Z.L. Li, H. Wu, B.H. Tang, L. Ma, E. Zhao, C. Li, Inversion of the PROSAIL model to estimate leaf area index of maise, potato, and sunflower fields from unmanned aerial vehicle hyperspectral data, International Journal of Applied Earth Observation and Geoinformation 26 (2014) 12–20, doi:10.1016/j.jag.2013.05.007.
[43] I. Kalisperakis, C. Stentoumis, L. Grammatikopoulos, K. Karantzalos, Leaf area index estimation in vineyards from UAV hyperspectral data, 2D image mosaics and 3D canopy surface models, The International Archives of the Photogrammetry, Remote Sensing and Spatial Information Sciences, XL-1/W4 (2015) 299–303, doi:10.5194/isprsarchives-xl-1-w4-299-2015.
[44] Z. Li, X. Jin, J. Wang, G. Yang, C. Nie, X. Xu, H. Feng, Estimating winter wheat (Triticum aestivum) LAI and leaf chlorophyll content from canopy reflectance data by integrating agronomic prior knowledge with the PROSAIL model, International Journal of Remote Sensing 36 (10) (2015) 2634–2653, doi:10.1080/01431161.2015.1041176.
[45] J. Yue, H. Feng, X. Jin, H. Yuan, Z. Li, C. Zhou, G. Yang, Q. Tian, A Comparison of Crop Parameters Estimation Using Images from UAV-Mounted Snapshot Hyperspectral Sensor and High-Definition Digital Camera, Remote Sensing 10 (7) (2018) 1138, doi:10.3390/rs10071138.
[46] Y. Zhao, S. Chen, S. Shen, Assimilating remote sensing information with crop model using Ensemble Kalman Filter for improving LAI monitoring and yield estimation, Ecological Modelling 270 (2013) 30–42, doi:10.1016/j.ecolmodel.2013.08.016.
[47] A.B. Potgieter, B. George-Jaeggli, S.C. Chapman, K. Laws, L.A. Suárez Cadavid, J. Wixted, J. Watson, M. Eldridge, D.R. Jordan, G.L. Hammer, Multi-Spectral Imaging from an Unmanned Aerial Vehicle Enables the Assessment of Seasonal Leaf Area Dynamics of Sorghum Breeding Lines, Frontiers in Plant Science 8 (2017), doi:10.3389/fpls.2017.01532.
[48] N.D. Mueller, J.S. Gerber, M. Johnston, D.K. Ray, N. Ramankutty, J.A. Foley, Closing yield gaps through nutrient and water management, Nature 490 (7419) (2012) 254–257, doi:10.1038/nature11420.
[49] G. Duveiller, M. Weiss, F. Baret, P. Defourny, Retrieving wheat Green Area Index during the growing season from optical time series measurements based on neural network radiative transfer inversion, Remote Sensing of Environment 115 (3) (2011) 887–896, doi:10.1016/j.rse.2010.11.016.
[50] J. Geipel, J. Link, W. Claupein, Combined Spectral and Spatial Modeling of Corn Yield Based on Aerial Images and Crop Surface Models Acquired with an Unmanned Aircraft System, Remote Sensing 6 (11) (2014) 10335–10355, doi:10.3390/rs61110335.
[51] A.D. Baez-Gonzalez, J.R. Kiniry, S.J. Maas, M.L. Tiscareno, C.J. Macias, J.L. Mendoza, C.W. Richardson, G.J. Salinas, J.R Manjarrez, Large-Area Maize Yield Forecasting Using Leaf Area Index Based Yield Model, Agronomy Journal 97 (2) (2005) 418–425, doi:10.2134/agronj2005.0418.
[52] A.A. Gitelson, G.P. Keydan, M.N. Merzlyak, Three-band model for noninvasive estimation of chlorophyll, carotenoids, and anthocyanin contents in higher plant leaves, Geophysical Research Letters (11) (2006) 33, doi:10.1029/2006gl026457.
[53] J.G.P.W. Clevers, L. Kooistra, Using Hyperspectral Remote Sensing Data for Retrieving Canopy Chlorophyll and Nitrogen Content, IEEE Journal of Selected Topics in Applied Earth Observations and Remote Sensing 5 (2) (2012) 574–583, doi:10.1109/jstars.2011.2176468.
[54] J.M. Hoeppner, A.K. Skidmore, R. Darvishzadeh, M. Heurich, H.C. Chang, T.W. Gara, Mapping Canopy Chlorophyll Content in a Temperate Forest Using Airborne Hyperspectral Data, Remote Sensing 12 (21) (2020) 3573, doi:10.3390/rs12213573.
[55] O. Mutanga, A. Skidmore, H. Prins, Predicting in situ pasture quality in the Kruger National Park, South Africa, using continuum-removed absorption features, Remote Sensing of Environment 89 (3) (2004) 393–408, doi:10.1016/j.rse.2003.11.001.
[56] C. Wu, Z. Niu, Q. Tang, W. Huang, Estimating chlorophyll content from hyperspectral vegetation indices: Modeling and validation, Agricultural and Forest Meteorology 148 (8–9) (2008) 1230–1241, doi:10.1016/j.agrformet.2008.03.005.
[57] R. Houborg, H. Soegaard, E. Boegh, Combining vegetation index and model inversion methods for the extraction of key vegetation biophysical parameters using Terra and Aqua MODIS reflectance data, Remote Sensing of Environment 106 (1) (2007) 39–58, doi:10.1016/j.rse.2006.07.016.
[58] R. Pu, S. Bell, C. Meyer, Mapping and assessing seagrass bed changes in Central Florida's west coast using multitemporal Landsat TM imagery, Estuarine, Coastal and Shelf Science 149 (2014) 68–79, doi:10.1016/j.ecss.2014.07.014.
[59] Y. Zhang, J.M. Chen, J.R. Miller, T.L. Noland, Leaf chlorophyll content retrieval from airborne hyperspectral remote sensing imagery, Remote Sensing of Environment 112 (7) (2008) 3234–3247, doi:10.1016/j.rse.2008.04.005.
[60] K.K. Wong, Y. He, Estimating grassland chlorophyll content using remote sensing data at leaf, canopy, and landscape scales, Canadian Journal of Remote Sensing 39 (2) (2013) 155–166, doi:10.5589/m13-021.
[61] M. Machwitz, R. Pieruschka, K. Berger, M. Schlerf, H. Aasen, S. Fahrner, J. Jiménez-Berni, F. Baret, U. Rascher, Bridging the Gap Between Remote Sensing and Plant Phenotyping—Challenges and Opportunities for the Next Generation of Sustainable Agriculture, Frontiers in Plant Science 12 (2021), doi:10.3389/fpls.2021.749374.
[62] S. Jacquemoud, W. Verhoef, F. Baret, C. Bacour, P.J. Zarco-Tejada, G.P. Asner, C. François, S.L. Ustin, PROSPECT+SAIL models: A review of use for vegetation characterization, Remote Sensing of Environment 113 (2009) S56–S66, doi:10.1016/j.rse.2008.01.026.
[63] B. Combal, F. Baret, M. Weiss, Improving canopy variables estimation from remote sensing data by exploiting ancillary information. Case study on sugar beet canopies, Agronomie 22 (2) (2002) 205–215, doi:10.1051/agro:2002008.
[64] A. Verger, F. Baret, F. Camacho, Optimal modalities for radiative transfer-neural network estimation of canopy biophysical characteristics: Evaluation over an agricultural area with CHRIS/PROBA observations, Remote Sensing of Environment 115 (2) (2011) 415–426, doi:10.1016/j.rse.2010.09.012.

[65] L. Liang, L. Di, L. Zhang, M. Deng, Z. Qin, S. Zhao, H. Lin, Estimation of crop LAI using hyperspectral vegetation indices and a hybrid inversion method, Remote Sensing of Environment 165 (2015) 123–134, doi:10.1016/j.rse.2015.04.032.
[66] F. Rossi, M. Nardino, P. Mannini, R. Genovesi, IRRINET Emilia Romagna: online decision support on irrigation. *Online agrometeological applications with decision support on the farm level*, Cost Action 718 (2004) 99–102.
[67] P. Mannini, R. Genovesi, T. Letterio, IRRINET: Large Scale DSS Application for On-farm Irrigation Scheduling, Procedia Environmental Sciences 19 (2013) 823–829, doi:10.1016/j.proenv.2013.06.091.
[68] R.J. Ritchie, Consistent Sets of Spectrophotometric Chlorophyll Equations for Acetone, Methanol and Ethanol Solvents, Photosynthesis Research 89 (1) (2006) 27–41, doi:10.1007/s11120-006-9065-9.
[69] C.R. Warren, Rapid Measurement of Chlorophylls with a Microplate Reader, Journal of Plant Nutrition 31 (7) (2008) 1321–1332, doi:10.1080/01904160802135092.
[70] M. Meroni, R. Colombo, C. Panigada, Inversion of a radiative transfer model with hyperspectral observations for LAI mapping in poplar plantations, Remote Sensing of Environment 92 (2) (2004) 195–206, doi:10.1016/j.rse.2004.06.005.
[71] S.T. Jagtap, K. Phasinam, T. Kassanuk, S.S. Jha, T. Ghosh, C.M. Thakar, Towards application of various machine learning techniques in agriculture, in: Materials Today: Proceedings, 2021, doi:10.1016/j.matpr.2021.06.236.
[72] E. Schulz, M. Speekenbrink, A. Krause, A tutorial on Gaussian process regression: Modelling, exploring, and exploiting functions, Journal of Mathematical Psychology 85 (2018) 1–16, doi:10.1016/j.jmp.2018.03.001.
[73] S.J. Gershman, D.M. Blei, A tutorial on Bayesian nonparametric models, Journal of Mathematical Psychology 56 (1) (2012) 1–12, doi:10.1016/j.jmp.2011.08.004.
[74] C.K.I. Williams, Prediction with Gaussian Processes: From Linear Regression to Linear Prediction and Beyond, Learning in Graphical Models (1998) 599–621, doi:10.1007/978-94-011-5014-9_23.
[75] A. Alexandros, A. Smola, K. Hornik, Kernel-Based Machine Learning Lab-Package 'kernlab', Springer, Berlin, Germany, 2019.
[76] J. Verrelst, Z. Malenovský, C. van der Tol, G. Camps-Valls, J.P. Gastellu-Etchegorry, P. Lewis, P. North, J. Moreno, Quantifying Vegetation Biophysical Variables from Imaging Spectroscopy Data: A Review on Retrieval Methods, Surveys in Geophysics 40 (3) (2018) 589–629, doi:10.1007/s10712-018-9478-y.
[77] J. Verrelst, S. Dethier, J.P. Rivera, J. Munoz-Mari, G. Camps-Valls, J. Moreno, Active Learning Methods for Efficient Hybrid Biophysical Variable Retrieval, IEEE Geoscience and Remote Sensing Letters 13 (7) (2016) 1012–1016, doi:10.1109/LGRS.2016.2560799.
[78] Wood, S.N. (2017) Generalized Additive Models: An Introduction with R (2nd edition). CRC/Taylor & Francis.
[79] K. Thorp, G. Wang, A. West, M. Moran, K. Bronson, J. White, J. Mon, Estimating crop biophysical properties from remote sensing data by inverting linked radiative transfer and ecophysiological models, Remote Sensing of Environment 124 (2012) 224–233, doi:10.1016/j.rse.2012.05.013.
[80] D.W. Lawlor, G. Cornic, Photosynthetic carbon assimilation and associated metabolism in relation to water deficits in higher plants, Plant, Cell & Environment 25 (2) (2002) 275–294, doi:10.1046/j.0016-8025.2001.00814.x.
[81] A. Ozbahce, A.F. Tari, Effects of different emitter space and water stress on yield and quality of processing tomato under semi-arid climate conditions, Agricultural Water Management 97 (9) (2010) 1405–1410, doi:10.1016/j.agwat.2010.04.008.
[82] E.J. Botha, B. Leblon, B. Zebarth, J. Watmough, Non-destructive estimation of potato leaf chlorophyll from canopy hyperspectral reflectance using the inverted PROSAIL model, International Journal of Applied Earth Observation and Geoinformation 9 (4) (2007) 360–374, doi:10.1016/j.jag.2006.11.003.
[83] L. Wan, J. Zhang, X. Dong, X. Du, J. Zhu, D. Sun, Y. Liu, Y. He, H. Cen, Unmanned aerial vehicle-based field phenotyping of crop biomass using growth traits retrieved from PROSAIL model, Computers and Electronics in Agriculture 187 (2021) 106304, doi:10.1016/j.compag.2021.106304.
[84] R. Darvishzadeh, A. Skidmore, M. Schlerf, C. Atzberger, Inversion of a radiative transfer model for estimating vegetation LAI and chlorophyll in a heterogeneous grassland, Remote Sensing of Environment 112 (5) (2008) 2592–2604, doi:10.1016/j.rse.2007.12.003.
[85] Q. Jiao, Q. Sun, B. Zhang, W. Huang, H. Ye, Z. Zhang, X. Zhang, B. Qian, A Random Forest Algorithm for Retrieving Canopy Chlorophyll Content of Wheat and Soybean Trained with PROSAIL Simulations Using Adjusted Average Leaf Angle, Remote Sensing 14 (1) (2021) 98, doi:10.3390/rs14010098.
[86] J.M. Chen, J. Liu, S.G. Leblanc, R. Lacaze, J.L. Roujean, Multi-angular optical remote sensing for assessing vegetation structure and carbon absorption, Remote Sensing of Environment 84 (4) (2003) 516–525, doi:10.1016/s0034-4257(02)00150-5.
[87] J.L. Widlowski, B. Pinty, N. Gobron, M.M. Verstraete, D.J. Diner, A.B. Davis, Canopy Structure Parameters Derived from Multi-Angular Remote Sensing Data for Terrestrial Carbon Studies, Climatic Change 67 (2–3) (2004) 403–415, doi:10.1007/s10584-004-3566-3.
[88] G. Antonucci, M. Croci, B. Miras-Moreno, A. Fracasso, S. Amaducci, Integration of Gas Exchange With Metabolomics: High-Throughput Phenotyping Methods for Screening Biostimulant-Elicited Beneficial Responses to Short-Term Water Deficit, Frontiers in Plant Science 12 (2021), doi:10.3389/fpls.2021.678925.
[89] E. Wozniak, A. Blaszczak, P. Wiatrak, M. Canady, Biostimulant Mode of Action, The Chemical Biology of Plant Biostimulants (2020) 205–227, doi:10.1002/9781119357254.ch8.
[90] Al Majathoub, M. (2004). Effect of biostimulants on production of wheat (Triticum aestivum L.). In: Mediterranean rainfed agriculture: Strategies for sustainability. Options Méditerranéennes: Série A. Séminaires Méditerranéens, vol. 60 (eds. C. Cantero-Martínez and D. Gabiña), 147–150. Zaragoza: CIHEAM.
[91] A. Grabowska, E. Kunicki, A. Sękara, A. Kalisz, R. Wojciechowska, The Effect of Cultivar and Biostimulant Treatment on the Carrot Yield and its Quality, Vegetable Crops Research Bulletin 77 (1) (2012) 37–48, doi:10.2478/v10032-012-0014-1.
[92] E. Kunicki, A. Grabowska, A. Sękara, R. Wojciechowska, The effect of cultivar type, time of cultivation, and biostimulant treatment on the yield of spinach (Spinacia oleracea L.), Folia Hortic 22 (2) (2010) 9.
[93] G. Colla, E. Svecova, M. Cardarelli, et al., Effectiveness of a plant-derived protein hydrolysate to improve crop performances under different growing conditions, Acta Hortic 1009 (2013) 175–179.
[94] A. Koukounaras, P. Tsouvaltzis, A.S. Siomos, Effect of root and foliar application of amino acids on the growth and yield of greenhouse tomato in different fertilization levels, J. Food Agric. Environ. 11 (2) (2013) 644–648.
[95] P. Mäkelä, K. Jokinen, M. Kontturi, P. Peltonen-Sainio, E. Pehu, S. Somersalo, Foliar application of glycinebetaine—a novel product from sugar beet—as an approach to increase (1998), doi:10.1016/s0926-6690(97)00042-3.
[96] S. Francesca, G. Raimondi, V. Cirillo, A. Maggio, A. Barone, M.M. Rigano, A Novel Plant-Based Biostimulant Improves Plant Performances under Drought Stress in Tomato, Biology and Life Sciences Forum 4 (1) (2020) 52, doi:10.3390/iecps2020-08883.